# Apoptosis induced by tungsten carbide-cobalt nanoparticles in JB6 cells involves ROS generation through both extrinsic and intrinsic apoptosis pathways

JINSHUN ZHAO[1,2], LINDA BOWMAN[2], RUTH MAGAYE[1], STEPHEN S. LEONARD[2], VINCENT CASTRANOVA[2] and MIN DING[2]

[1]Department of Preventive Medicine of the Medical School, Zhejiang Provincial Key Laboratory of Pathological and Physiological Technology, Ningbo University, Ningbo, Zhejiang 315211, P.R. China; [2]Pathology and Physiology Research Branch, Health Effects Laboratory Division, National Institute for Occupational Safety and Health, Morgantown, WV 26505, USA

**Abstract.** In this study, apoptosis and related signaling induced by WC-Co nanoparticles were investigated in JB6 cells and rat lung macrophages. Electron spin resonance (ESR) and fluorescent staining indicated that both WC-Co nanoparticles and fine particles stimulated reactive oxygen species (ROS) generation. Catalase exhibited an inhibitory effect on WC-Co nanoparticle-induced ROS as well as mitochondrial membrane permeability damage. Further study indicated that WC-Co nanoparticles elicited higher cytotoxicity and apoptotic induction than fine particles. Western blot analysis showed activation of proapoptotic factors including Fas, Fas-associated protein with death domain (FADD), caspase 3, 8 and 9, BID and BAX. In addition, both cytochrome $c$ and apoptosis-inducing factor (AIF) were upregulated and released from mitochondria to the cytoplasm. Our findings demonstrate that, on a mass basis, WC-Co nanoparticles exhibit higher cytotoxicity and apoptotic induction than fine particles. Apoptosis induced by WC-Co nanoparticles and fine particles involves both extrinsic and intrinsic apoptosis pathways.

*Correspondence to:* Professor Jinshun Zhao, Department of Preventive Medicine of the Medical School, Zhejiang Provincial Key Laboratory of Pathological and Physiological Technology, Ningbo University, 818 Fengua Road, Jiangbei District, Ningbo, Zhejiang 315211, P.R. China
E-mail: zhaojinshun@nbu.edu.cn

Dr Min Ding, Pathology and Physiology Research Branch, Health Effects Laboratory Division, National Institute for Occupational Safety and Health, 1095 Willowdale Road, Morgantown, WV 26505, USA
E-mail: mid5@cdc.gov

## Introduction

Nano-scale particle research has recently become a very important field in materials science. Nanoparticles (1 to 100 nm) usually have physical properties different from those of large particles (1-10 $\mu$m). It has been found that nanoparticles exhibit a variety of novel properties, depending on particle size, including magnetic, optical, and other physical properties as well as surface reactivity (1). Hard metals consisting of tungsten carbide (WC) and metallic cobalt (Co) particles are important industrial materials (2). WC-Co nanoparticle composites have the potential to replace standard materials for tools and wear parts because of their increased hardness and toughness. By means of particle size reduction, the fracture toughness and wear resistance of WC-Co can be increased significantly. Research evidence indicated that WC-Co fine particle mixture was carcinogenic in exposed workers (2). Based on the fact that nanoparticles of metallic nickel and titanium dioxide (TiO$_2$) cause more pronounced toxicity than fine particles (3-7), the pathogenic effects of WC-Co particles may well vary with their size.

Among the possible mechanisms of metal toxicity, apoptosis plays an important role in carcinogenesis (8). While a number of known or suspected human carcinogenic metallic compounds have been shown to induce apoptosis, the relevance of these observations for the carcinogenic process is, however, still not completely understood (9). Apoptosis induced by WC-Co fine particles has been reported in previous *in vitro* studies (2,9); however, the signal pathways induced by WC-Co particles still remain elusive.

Apoptosis is a highly regulated process that is involved in physiological as well as pathological conditions (10-13). Deregulation of apoptosis has been implicated in carcinogenesis, tumor progression and resistance of tumor cells to radio- and chemotherapy (14,15). Malfunction of apoptosis plays an important role in many disease processes. An inefficient elimination of mutated cells may favor carcinogenesis or tumorigenesis; failure to clear inflammatory cells may prolong the inflammation because of the release of damaging histotoxins (9). However, excessive apoptosis has been shown

to contribute to pulmonary fibrosis in mice (16). Furthermore, enhanced apoptosis may indirectly trigger compensatory cell proliferation to ensure tissue homeostasis and promote the fixation of mutagenic events or multiplication of mutated cells. Studies have demonstrated that apoptosis is also involved in pulmonary disorders, such as acute lung injury, diffuse alveolar damage, idiopathic pulmonary fibrosis, and other lung disorders caused by bleomycin, silica, endotoxins, and the deposition of immune complexes (16-19). Inhibition of apoptosis by gene deletion strategies or by caspase inhibitors abrogate the pathologic effects of these agents (16-20), supporting the potential role of apoptosis in the inflammatory, pulmonary fibrosis, and immunopathologic disorders. Therefore, the apoptotic properties may be important for elucidating the mechanisms of adverse health effects induced by WC-Co particles.

Accordingly, the objectives of this study are to compare the difference in cytotoxicity and apoptosis induced by WC-Co nano- and fine particles, and to elucidate the mechanisms of cell death induced by WC-Co particles. This study provides insight into the role of apoptosis in the possible pathogenicity and carcinogenicity induced by WC-Co nanoparticles.

**Materials and methods**

*Materials*. WC-Co nanoparticles (99.9% pure, molecularly mixed at the ratio of 85:15, agglomerated powder) were purchased from Inframat® Advanced Materials™ LLC (Farmington, CT, USA). WC-Co fine particles were purchased from Alfa ASAR. Eagle's minimal essential medium (EMEM) was obtained from Lonza (Walkersville, MD). Fetal bovine serum (FBS), trypsin, pencillin/streptomycin and L-glutamine were purchased from Life Technologies Inc. (Gaithersburg, MD). YO-PRO-1 [YP, 1 mM solution in dimethyl sulfoxide (DMSO)] and propidium iodide (PI, 1.0 mg/ml in water) were purchased from Invitrogen (Carlsbad, CA). Hoechst 33342, 2', 7'-dichlorodihydrofluorescein diacetate (H2DCFDA) and dihydroethidium (DHE) were purchased from Molecular Probes (Eugene, OR). Anti-h/m caspase-8 antibody was obtained from R&D Systems (Minneapolis, MN). BID and cleaved caspase 3 antibodies were purchased from Cell Signaling Technology (Beverley, MA). All other antibodies were obtained from Santa Cruz Biotechnology Co. (Santa Cruz, CA). Cell proliferation kit I (MTT assay kit) was obtained from Roche Applied Science (Penzberg, Germany). Mitochondria Staining Kit and catalase were purchased from Sigma-Aldrich (Saint Louis, MO).

*Preparation of WC-Co particles*. Stock solutions of WC-Co nano- or fine particles were prepared by sonication on ice using a Branson Sonifier 450 (Branson Ultrasonics Corp., Danbury, CT) in sterile PBS (10 mg/ml) for 30 sec, then kept on ice for 15 sec and sonicated again for a total of 3 min at a power of 400 W. Before use, these particles were diluted to a designed concentration in fresh culture medium. All samples were prepared under sterile conditions.

*Surface area and size distribution measurements*. Surface area of WC-Co particles was measured using the Gemini 2360 Surface Area Analyzer (Mircomeritics, Norcross, GA) with a flowing gas technique according to the manufacturer's instructions. The size distribution of WC-Co particles was detected using scanning electron microscopy (SEM). Briefly, WC-Co particles were prepared by sonication. Then, the samples were diluted in double-distilled water and air dried onto a carbon planchet. Images were collected on a scanning electron microscope (Hitachi S-4800, Japan) according to the manufacturer's instructions. Optimas 6.5 image analysis software (Media Cybernetics, Bethesda, MD) was used to measure the diameter of WC-Co particles.

*Cell culture*. Mouse epidermal JB6 cells were maintained in 5% FBS EMEM containing 2 mM L-glutamine and 1% penicillin-streptomycin (10,000 U/ml penicillin and 10 mg/ml streptomycin) at standard culture conditions (37°C, 80% humidified air and 5% $CO_2$). For all treatments, cells were grown to 80% confluence.

*Determination of free radical formation*. All ESR measurements were conducted using a Varian E9 ESR spectrometer and a flat cell assembly. Hyperfine couplings were measured (to 0.1 G) directly from magnetic field separation using potassium tetraperoxochromate ($K_3CrO_8$) and 1,1-diphenyl-2-picrylhydrazyl as reference standards. An EPR DAP 2.0 program was used for data acquisition and analyses. Reactants were mixed in test tubes in a total final volume of 450 $\mu$l. The reaction mixture was then transferred to a flat cell for ESR measurement. The concentrations given in the figure legends are final concentrations and measurements were made at room temperature and under ambient air, except those specifically indicated otherwise. The receiver gain, time constant, sweep time, sweep width, modulation frequency, modulation amplitude and microwave power were set constant to allow relative intensity comparisons of spectra. All spectra shown are the accumulation of five scans. Hyperfine couplings constants were determined using the WinSim program of the NIEHS public EPR software tools, available over the internet (http://epr.niehs.nih.gov). The relative radical concentration was estimated by measuring the peak-to-peak height (mm) of the observed spectra.

H2DCFDA and DHE are used for staining general ROS or oxygen radicals ($\bullet O_2^-$) produced in intact cells, respectively. Hoechst 33342 is a nucleic acid stain. JB6 cells were seeded into a 24-well plate. Cells were grown 24 h and then starved in 0.1% FBS EMEM overnight. Cells were then treated with/without various concentrations of WC-Co nano- or fine particles in the presence of H2DCFDA (5 $\mu$M), DHE (2 $\mu$M) and Hoechst 33342 (3 $\mu$M) for 1 h. The cells were washed 3 times with PBS, followed by addition of fresh 0.1% FBS EMEM. The images were captured with a fluorescence microscope (Axiovert 100M, Zeiss, Germany).

*Cytotoxicity assay*. Cytotoxicity of WC-Co particles to JB6 cells was assessed by an MTT assay kit following the manufacturer's instructions. Briefly, cells were plated in 100 ml EMEM at a density of $10^4$ cells/well in a 96-well plate. The cells were grown for 24 h and then, treated with various concentrations of WC-Co particles. After 24-h incubation, 10 ml MTT labeling reagent was added in each well and the plates were further incubated for 4 h. Afterward, 100 ml solubilization solution was added to each well and the plate was incubated overnight at 37°C. The optical density (OD) of the wells was measured at a wavelength of

575 nm with reference of 690 nm using an ELISA plate reader. Results were calculated using the OD measured without cells.

*Detection of apoptosis.* YP staining was used to detect cell apoptosis in JB6 cells. Briefly, cells were seeded onto a 24-well plate overnight. Then, cells were treated with/without various concentrations of WC-Co nano- or fine particles for 24 h. Before microscopy, YP dye was added into the cultures (10 $\mu$g/ml) and cells were further incubated for 1 h. Then, cells were washed two times with EMEM medium. Apoptotic cells were monitored using a fluorescent microscope (Axiovert 100M). Percentage of cells exhibiting apoptosis was calculated.

*Sub-cellular fractionation and western blot analysis.* Briefly, cells were plated onto a 100x20 mm cell culture dish. The cultures were grown for 24 h and then starved in 0.1% FBS EMEM overnight. Cells were treated with/without WC-Co nano- or fine particles. After treatment, the cells were extracted with 1X SDS sample buffer supplemented with protease inhibitor cocktail (Sigma-Aldrich). Protein concentrations were determined using the bicinchoninic acid method (Pierce, Rockford, IL). Equal amounts of proteins were separated by 4-12% Tris glycine gels. Immunoblots for expression of Fas, FADD, caspase 3, caspase 8, caspase 9, BID, cleaved BID, BAX, Bcl-2, cytochrome *c*, AIF, lamin A/C, $\beta$-actin and $\beta$-tubulin were detected. Experiments were performed three or more times, and equal loading of protein was ensured by measuring $\beta$-actin and $\beta$-tubulin expression.

To prepare the subcellular fractionation, after treatment cells were washed twice with cold PBS. Then, cells were resuspended in 50 $\mu$l 1X Cytosol Extraction Buffer Mix and incubated on ice for 10 min. Cells were homogenized by passing through 22-gauge needles 30 times. The lysate was centrifuged at 700 x g for 10 min at 4°C to remove unbroken cells and nuclei. The supernatant was then re-centrifuged at 10,000 x g for 30 min at 4°C. The resulting supernatant was the cytosolic fraction while the pellet contained mitochondria. The cytosolic fraction was diluted using 50 $\mu$l of 2X SDS sample buffer. The mitochondrial pellet was resuspended in 20 $\mu$l Mitochondria Extraction Buffer Mix plus 20 $\mu$l of 2X SDS sample buffer. These two different fractions were used for western blot analysis.

*Detection of mitochondrial membrane permeability.* JB6 cells were seeded onto a 24-well plate overnight. Cells were treated with/without WC-Co nano- or fine particles supplemented with or without catalase (10,000 U/ml) for 24 h. Changes in mitochondrial membrane permeability were evaluated using a mitochondrial staining kit (JC1 staining) according to the manufacturer's instructions. Briefly, a staining mixture was prepared by mixing the staining solution with an equal volume of the EMEM medium. Cells were incubated in the staining mixture (0.4 ml/well) for 30 min at 37°C in a humidified atmosphere containing 5% $CO_2$. Thereafter, cells were washed two times in medium, followed by addition of fresh medium. Mitochondrial membrane permeability was monitored on a fluorescence microscope (Axiovert 100M).

*Isolation of rat lung macrophages.* Brown Norway rats were obtained from Charles River Laboratories (Wilmington, MA). The animals were housed in AAALA-accredited facility,

specific-pathogen-free, environmentally controlled facility located at National Institute for Occupational Safety and Health (Morgantown, WV). The rats were monitored to be free of endogenous viral pathogens, parasites, *mycoplasma*, *helicobacter* and CAR *Bacillus*. Rats were acclimated for at least 5 days before use, and were housed in ventilated cages that were provided with HEPA-filtered air, with $\alpha$-Dri virgin cellulose chips and hardwood $\beta$-chips used as bedding. The rats were maintained on ProLab 3500 diet and tap water, both of which were provided *ad libitum*. Rats were anesthetized using brevital sodium (40 mg/kg), and exposed to 100 $\mu$l/rat of 1% WC-Co nanoparticles suspended in sterile saline (100 $\mu$l of saline for control rat) by intranasal droplet application 4 times (totally 4 g/rat) on day 0, 7, 14 and 21, respectively. At 24 h after the last treatment, rats were sacrificed by intraperitoneal injection of 0.2 g/kg pentobarbital, and then the descending aorta was cut. The trachea was exposed, and a cannula was inserted. Bronchoalveolar lavage fluid (BALF) was collected using saline. After centrifugation, cells in BALF were seeded into a 6-well plate in 5% FBS EMEM containing 2 mM L-glutamine and 1% penicillin-streptomycin (10,000 U/ml penicillin and 10 mg/ml streptomycin) at standard culture conditions (37°C, 80% humidified air and 5% $CO_2$). After 4-h incubation, the unattached cells were washed out by using 5% FBS EMEM for 3 times. Attached cells (rat lung macrophages) were used for mitochondrial membrane permeability or apoptotic detections. Mitochondrial membrane permeability of rat lung macrophages was evaluated using a mitochondrial staining kit according to the manufacturer's instructions as stated above.

*Apoptotic detection of rat lung macrophages.* Dual staining using YP and PI were used to distinguish between apoptosis and necrosis (or late apoptosis) as described previously (21,22) with some modifications. Rat lung macrophages were obtained as stated above. YP and PI were added into the cultures with a final concentration of 10 $\mu$g/ml and 1 $\mu$M, respectively. Thereafter, rat lung macrophages were incubated in 5% FBS EMEM medium containing YP and PI dyes at 37°C in a humidified atmosphere containing 5% $CO_2$ for 1 h. Then, cells were washed two times in medium, followed by addition of fresh medium. Apoptotic cells were monitored using a fluorescence microscope (Axiovert 100M). YP stained cells were detected with a blue excitation filter. PI stained cells were measured using a green excitation filter.

*Statistical analysis.* Data are presented as means ± standard errors (SE) of the number of experiments/samples. Data were analyzed using one-way analysis of variance (ANOVA). Significance was set at p≤0.05.

## Results

*Surface area and size distribution of WC-Co particles.* Gemini 2360 Surface Area Analyzer and scanning electron microscopy were used to measure the surface area and size distribution of WC-Co particles, respectively. The average surface area of WC-Co nano and fine particles were published previously (23). The average surface area of WC-Co nanoparticles was 2.73 $m^2$/g compared to 0.16 $m^2$/g for fine particles. The average size distribution of WC-Co nano- and fine particles is 95.53 nm and 39.00 $\mu$m, respectively.
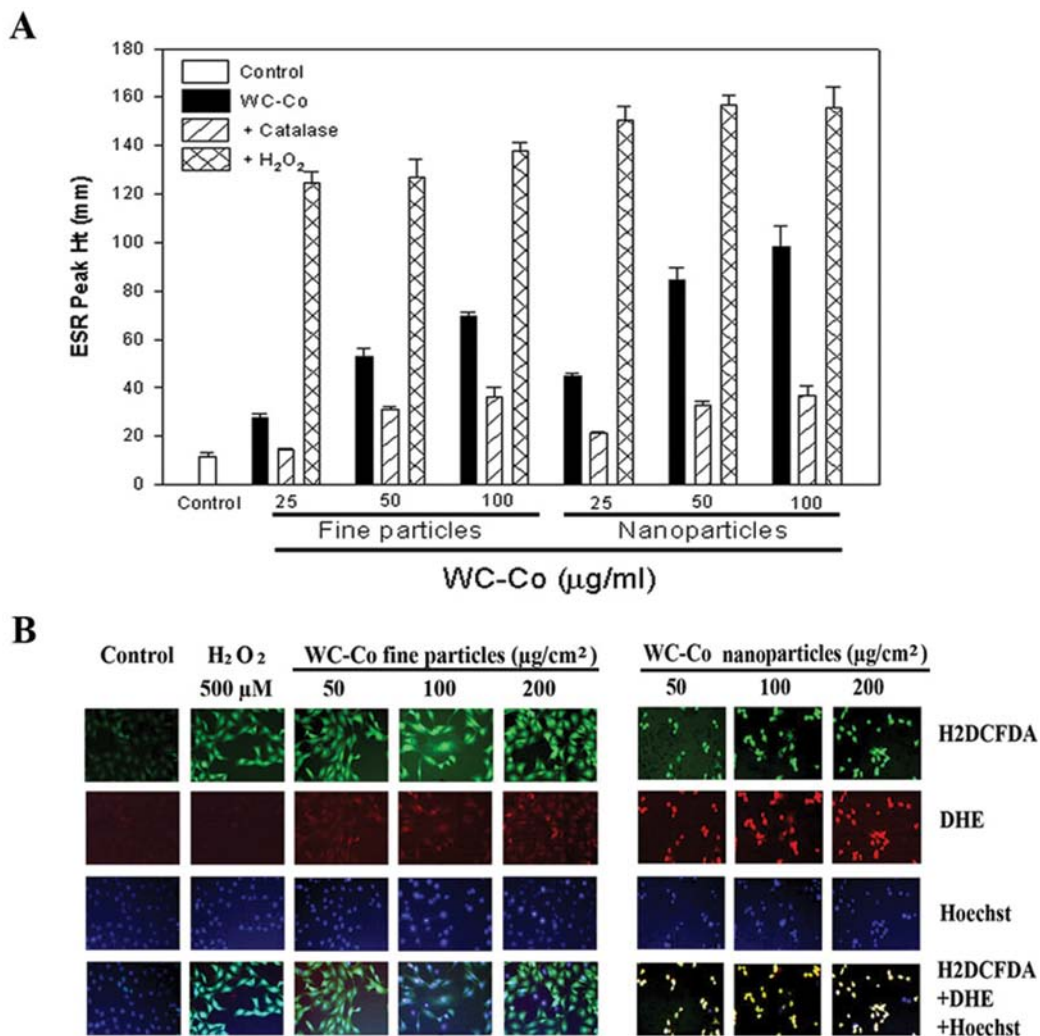
Figure 1. Free radical generation induced by WC-Co particles in JB6 cells. ESR and fluorescence staining were used to examine free radical generation induced by WC-Co particles as well as interactions of catalase or hydrogen peroxide with WC-Co particles in JB6 cells. (A) JB6 cells ($1 \times 10^6$ cells) in PBS (pH 7.4) plus 200 mM DMPO were treated with or without WC-Co particles plus catalase or hydrogen peroxide, OH- radical generation was measured by ESR. Instrument conditions: microwave power, 126 mW; modulation amplitude, 1.0 G; time constant, 40.96 msec; conversion time, 40.96 msec. Experiments were performed at room temperature. (B) JB6 cells were treated with various concentrations of WC-Co nano- or fine particles in the presence of 5 $\mu$M H2DCFDA, 2 $\mu$M DHE and 3 $\mu$M Hoechst 33342 for 1 h. The cells were washed 3 times with PBS followed by addition of fresh medium. The images were captured with a fluorescence microscope. The green color in the cells represents oxidized H2DCFDA, and the red color represents oxidized DHE indicating the intracellular localization of general free radicals or $\bullet O_2^-$, respectively. The blue color stained by Hoechst 33342 represents nuclear localization. $H_2O_2$ (50 $\mu$M) was used as a positive control.

*Free radical generation induced by WC-Co particles in JB6 cells.* The ESR spin trapping technique and fluorescent staining were used to detect free radical generation during incubation of WC-Co nano- or fine particles with JB6 cells (Fig. 1). Using the ESR spin trapping technique, we observed the formation of free radicals in JB6 cells exposed to WC-Co nano- or fine particles. After 5 min exposure of JB6 cells to WC-Co particles, DMPO radical adducts were recorded. The ESR signal from WC-Co nanoparticles was much stronger than fine particles (Fig. 1A). Addition of catalase, an $H_2O_2$ scavenger decreased the radical generation, while addition of $H_2O_2$ dramatically increased the ROS adduct signal (Fig. 1A). These results suggest that ROS generated during exposure of WC-Co particles to JB6 cells was formed via a metal-dependent Fenton reaction. H2DCFDA, a general ROS sensitive dye, and DHE, an $\bullet O_2^-$ specific dye, were used to monitor ROS generation induced by WC-Co particles

in intact cells. Hoechst 33342 was used for nucleic localization. Results showed that WC-Co nanoparticles induced stronger ROS generation, indicated by DHE staining, compared to fine particles (Fig. 1B).

*Effects of WC-Co particles on cell viability and apoptotic induction.* To determine whether there is a difference in the cytotoxicity induced by different sizes of WC-Co particles, various concentrations (5-100 $\mu$g/cm$^2$) of WC-Co nano- or fine particles were used to study the effects on cell viability in JB6 cells using the MTT assay (Fig. 2). After 24-h treatment, both WC-Co nano- and fine particles caused a dose-dependent cytotoxicity in JB6 cells (Fig. 2A). Cytotoxicity induced by WC-Co nanoparticles was significantly higher than fine particles between the concentration of 40 and 100 $\mu$g/cm$^2$. To detect apoptosis induced by WC-Co particles, YP staining
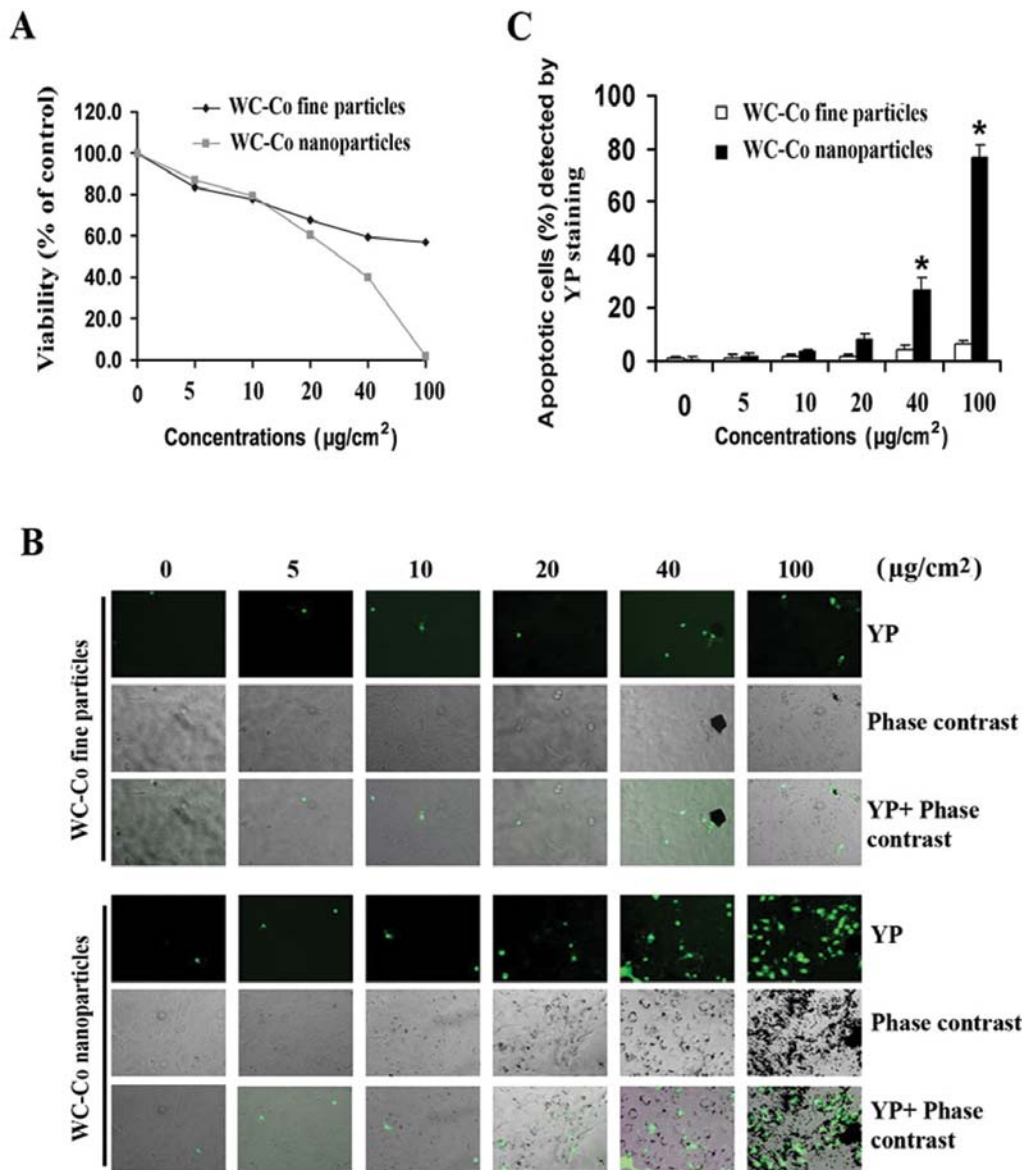
Figure 2. Cytotoxicity and apoptosis induced by WC-Co particles in JB6 cells. JB6 cells were seeded onto a 96- or 24-well plate and incubated overnight. Cells were treated with or without various concentrations of WC-Co nano- or fine particles for 24 h. Effects of WC-Co particles on cell viability (in a 96-well plate) and apoptotic induction (in a 24-well plate) were detected. (A) Cell viability was detected using the MTT assay. Data shown are means of three independent assays. (B) Apoptotic cells were stained by YP dye and monitored using a fluorescence microscope (x10 magnification). (C) Percentage of cells exhibiting apoptosis was calculated. WC-Co nanoparticles induced more cytotoxicity and apoptosis than fine particles at 40 and 100 $\mu g/cm^2$ analyzed by Student's t-test (p<0.05) indicated by *. Data shown are means ± SE of three independent assays.

was used. Results indicated that both WC-Co nano- and fine particles induced JB6 cell apoptosis (Fig. 2B). The percentage of apoptotic cells was significantly higher in cells treated with nanoparticles than fine particles between the concentration of 40 and 100 $\mu g/cm^2$. At the concentration of 100 $\mu g/cm^2$, there was an 8-fold increase in apoptosis induced by nanoparticles compared to fine particles (Fig. 2C).

*Effects of WC-Co particles on Fas, FADD, caspase 3, 8 and 9, lamin A/C, BID, BAX and Bcl-2.* To investigate the involvement of extrinsic signals in the apoptotic process induced by WC-Co particles, expression of Fas and FADD was examined. JB6 cells were treated with WC-Co nano- or fine particles (100 $\mu g/cm^2$) for 1, 3, 6 and 8 h, respectively, and then the protein expression

patterns were detected by western blot analysis (Fig. 3). Results demonstrated that WC-Co nano- and fine particles, especially nanoparticles, stimulated Fas and FADD expression.

Caspases are a family of cysteine proteases which play essential roles in apoptosis, necrosis and inflammation (24). Eleven caspases have been identified in humans. There are two types of apoptotic caspases: initiator caspases and effector caspases. Initiator caspases (e.g. caspase 8) cleave inactive pro-forms of effector caspases, thereby activating them. Effecter caspases (e.g. caspase 3) in turn cleave other protein substrates resulting in the apoptotic process. Our results indicated that caspase 3 and 8 were significantly cleaved and a slight activation of caspase 9 was observed. BAX and BID, two proapoptotic members of Bcl-2 family, were upregulated by WC-Co particles. Bcl-2,
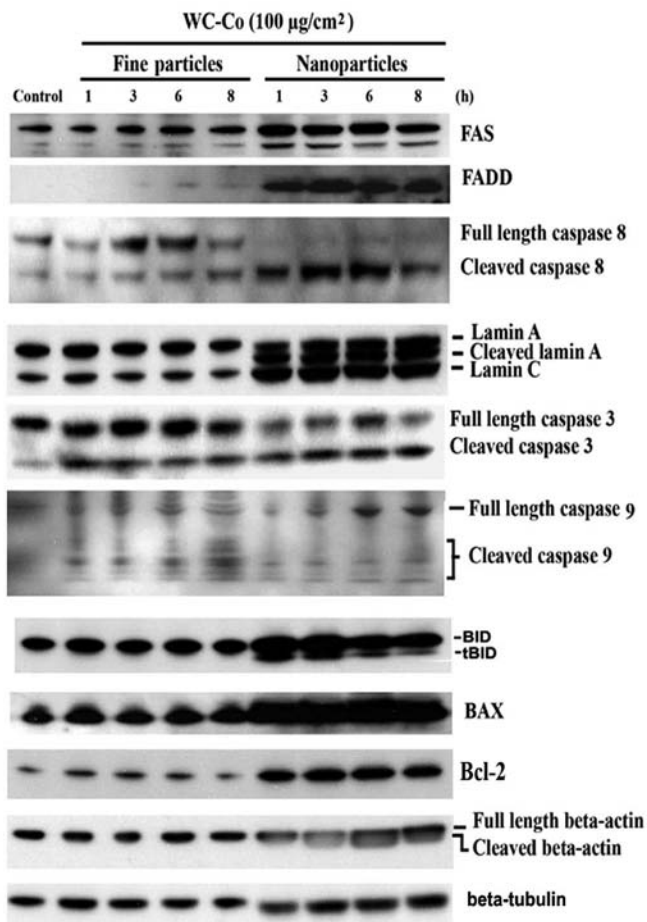
Figure 3. Effects of WC-Co particles on Fas, FADD, caspase 3, 8 and 9, lamin A/C, BAX, BID and Bcl-2. JB6 cells were seeded onto a culture dish and incubated overnight. Cells were treated with 100 $\mu g/cm^2$ WC-Co nano- or fine particles for 1, 3, 6 and 8 h. Expressions of Fas, FADD, caspase 3, 8, and 9, lamin A/C, BAX, BID and Bcl-2 were analyzed by western blot analysis. Expression of β-tubulin was set as a protein loading control.

an anti-apoptotic factor, was also upregulated. The cellular morphology associated with the apoptotic process has been well characterized by membrane blebbing, formation of apoptotic bodies, and chromosome condensation. These apoptotic changes are the result of the cleavage of cellular proteins, such as lamin and actin (25,26). In this study, cleavage of lamin A and β-actin were observed, especially in cells treated with WC-Co nanoparticles. The cleavage of lamin A and β-actin were detected as early as 1 h post-exposure of WC-Co nanoparticles. Interestingly, WC-Co nanoparticles induced lamin C upregulation without cleavage.

*Effects of WC-Co particles on cytochrome c and AIF.* The intrinsic pathway of apoptosis is initiated in the mitochondria. Its activation involves release of cytochrome *c* and other proapoptotic factors from the mitochondrial intermembrane space (27). AIF is a proapoptotic factor, a mitochondrial protein (28). It is normally confined to the mitochondrial intermembrane space (29). After release from mitochondria into the cytoplasm, both cytochrome *c* and AIF can stimulate cell apoptosis by initiating the intrinsic pathway. To test the effects of WC-Co particles on the intrinsic pathway of apoptosis, JB6 cells were

treated with nano- or fine particles (100 $\mu g/cm^2$) for 1, 3, 6 and 8 h, respectively. Western blots revealed that both nano- and fine particles induced cytochrome *c* and AIF upregulation as well as release from mitochondria to the cytoplasm after 1 h treatment, with nano-WC-Co exhibiting greater potency (Fig. 4A).

*Effects of WC-Co particles on mitochondrial membrane permeability.* Mitochondrial membrane permeability change is a hallmark for apoptosis (30). JB6 cells were treated with or without various concentrations of WC-Co particles for 24 h. Mitochondrial membrane permeability was evaluated using a JC-1 staining kit according to the manufacturer's instructions. The results indicated that both WC-Co nano- and fine particles induced a significant change in the mitochondrial membrane permeability compared to control, with nano WC-Co exhibiting greater potency. Valinomycin (1 $\mu l/ml$ culture medium) and $H_2O_2$ (500 $\mu M$) for 1 h were used as positive controls and Hoechst 33342 was used for nucleic localization (Fig. 4B).

*Effect of catalase on WC-Co particle-induced mitochondrial membrane permeability alteration.* According to the results obtained above as well as our previous studies (23), ROS may play an important role in WC-Co particle-induced mitochondrial membrane permeability alteration. To verify this hypothesis, the inhibitory effect of catalase on WC-Co particle-induced mitochondrial membrane permeability alteration was examined by using a mitochondrial staining kit (Fig. 5). The results showed that catalase could slightly inhibit any WC-Co particle-induced mitochondrial membrane permeability damage. In addition, catalase significantly inhibited mitochondrial membrane permeability damage induced by $H_2O_2$ (a free radical-apoptotic reagent), but not by valinomycin (a non-free radical-apoptotic reagent).

*Apoptosis and mitochondrial membrane permeability alteration induced by WC-Co nanoparticles in rat lung macrophages.* Apoptosis and mitochondrial membrane permeability alteration induced by WC-Co nanoparticles in rat lung macrophages were investigated as described in Materials and methods. Results indicated that lung macrophages from WC-Co nanoparticle-treated rats exhibited more apoptosis and mitochondrial membrane permeability damage compared to control (Fig. 6).

## Discussion

With the increased use of nanoparticles in modern industries, inhaled nanoparticles are increasingly being recognized as a potential health threat (31). Hard metal, a mixture of WC-Co, is an important industrial material. Occupational exposure of workers to the WC-Co particle mixture has been shown to be carcinogenic, and Co itself can also induce occupational asthma (32). WC-Co nanoparticles were introduced in industry (33) to improve hardness and toughness compared to standard WC-Co materials. The increasing use of WC-Co nanoparticles may lead to an increased human exposure and adverse health effects (34). The International Agency for Research on Cancer (IARC) has classified Co and its compounds as possibly carcinogenic to humans (35). However, the molecular mechanisms involved in hard metal-induced
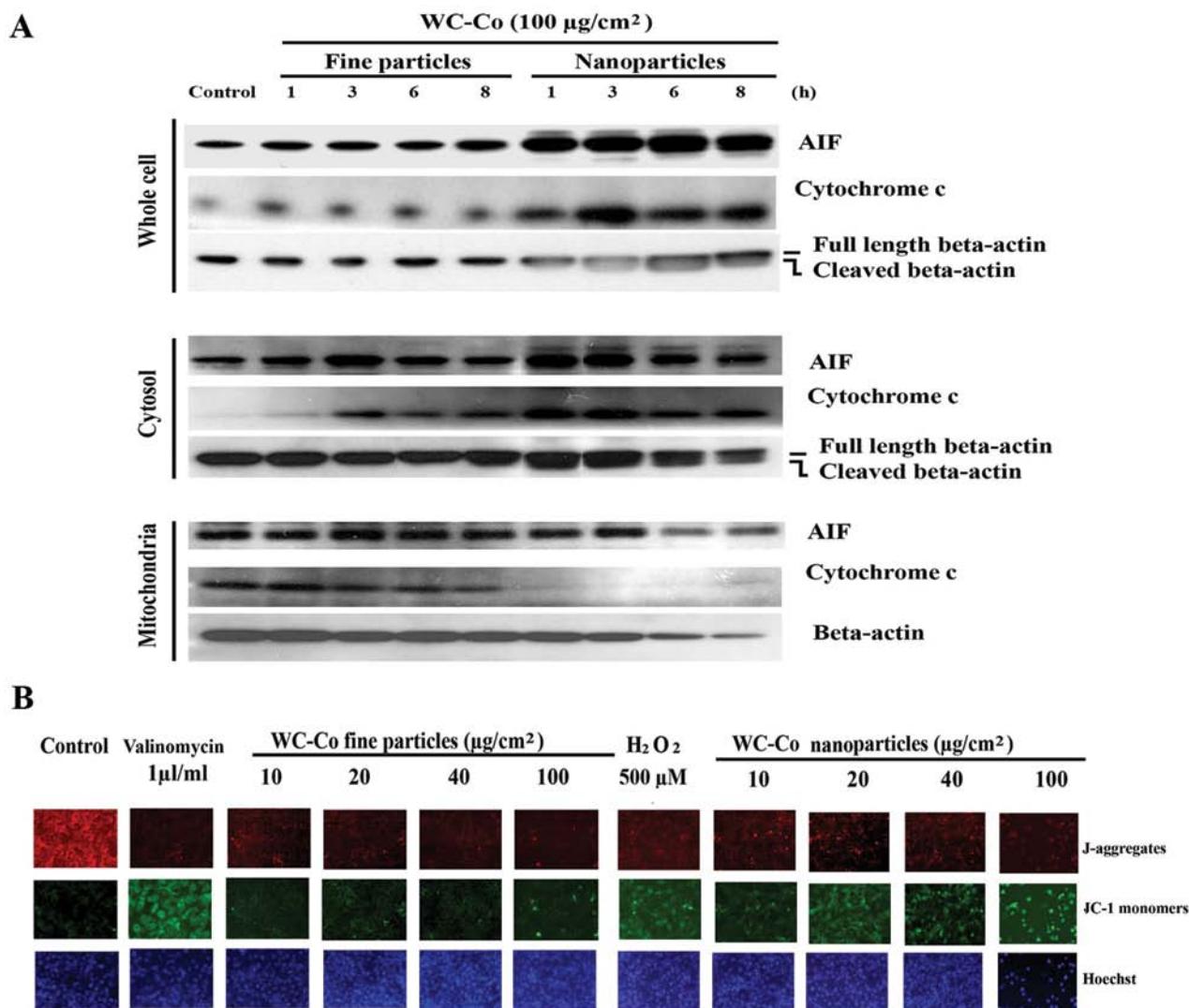
Figure 4. Effect of WC-Co particles on mitochondrial membrane permeability. Effects of WC-Co particles on mitochondrial membrane permeability were detected by both western blot and mitochondrial staining assay. (A) Cells were treated with 100 $\mu$g/cm$^2$ WC-Co nano- or fine particles for 1, 3, 6 and 8 h. Whole cell lysate or subcellular fractionations were prepared. Expressions of cytochrome $c$ and AIF in whole cell, cytosol or mitochondrial lysate were detected by western blot analysis. WC-Co particles, especially nanoparticles, markedly induced cytochrome $c$ and AIF upregulation and release from mitochondria into the cytoplasm. β-actin was cleaved. (B) JB6 cells were seeded onto a 24-well plate and incubated overnight. Cells were treated with or without various concentrations of WC-Co nano- or fine particles for 24 h. A mitochondrial staining kit was used to detect the mitochondrial membrane permeability. WC-Co particles induced significant change in the mitochondrial membrane permeability compared to negative control after 24 h treatment. Treatments with H$_2$O$_2$ (500 $\mu$M) for 24 h or valinomycin (1 $\mu$l/ml culture medium) for 1 h were used as positive control.

carcinogenesis are unclear. In addition, the health effects of occupational exposure to WC-Co nanoparticles are unknown. The molecular events mediating cellular responses to WC-Co particles also remain to be elucidated.

It is well known that the toxicity of particles to the lung in both occupational and environmental settings is not only related to exposure but also to the particle size. We have previously shown that nanoparticles of TiO$_2$ and metallic nickel produce higher cytotoxicity than their conventional fine particles, respectively (6,7). Accordingly, WC-Co nanoparticles may be more toxic than WC-Co fine particles.

In this study, we observed that both WC-Co nano- and fine particles induced ROS generation in a dose-dependent manner. This result is in agreement with our previous study which indicated that compared to fine particle WC-Co nanoparticles

generated a higher level of free radicals and induced greater oxidative stress, as evidenced by a decrease of GSH levels (23). Further studies indicated that catalase inhibits WC-Co particle-induced mitochondrial membrane permeability damage in JB6 cells. These results demonstrate that hydrogen peroxide may play an important role in the pathogenicity induced by WC-Co particles.

Using MTT and apoptotic assays, we observed that both WC-Co nano- and fine particles were cytotoxic in JB6 cells, while nanoparticles showed higher cytotoxicity and apoptotic induction than fine particles. In an inhalation study in rats, Oberdoerster et al demonstrated TiO$_2$ nanoparticles to be more inflammatory than fine TiO$_2$ particles (4). However, when normalized to surface area, they found that the dose-response curves for the nano- and fine particles were similar,
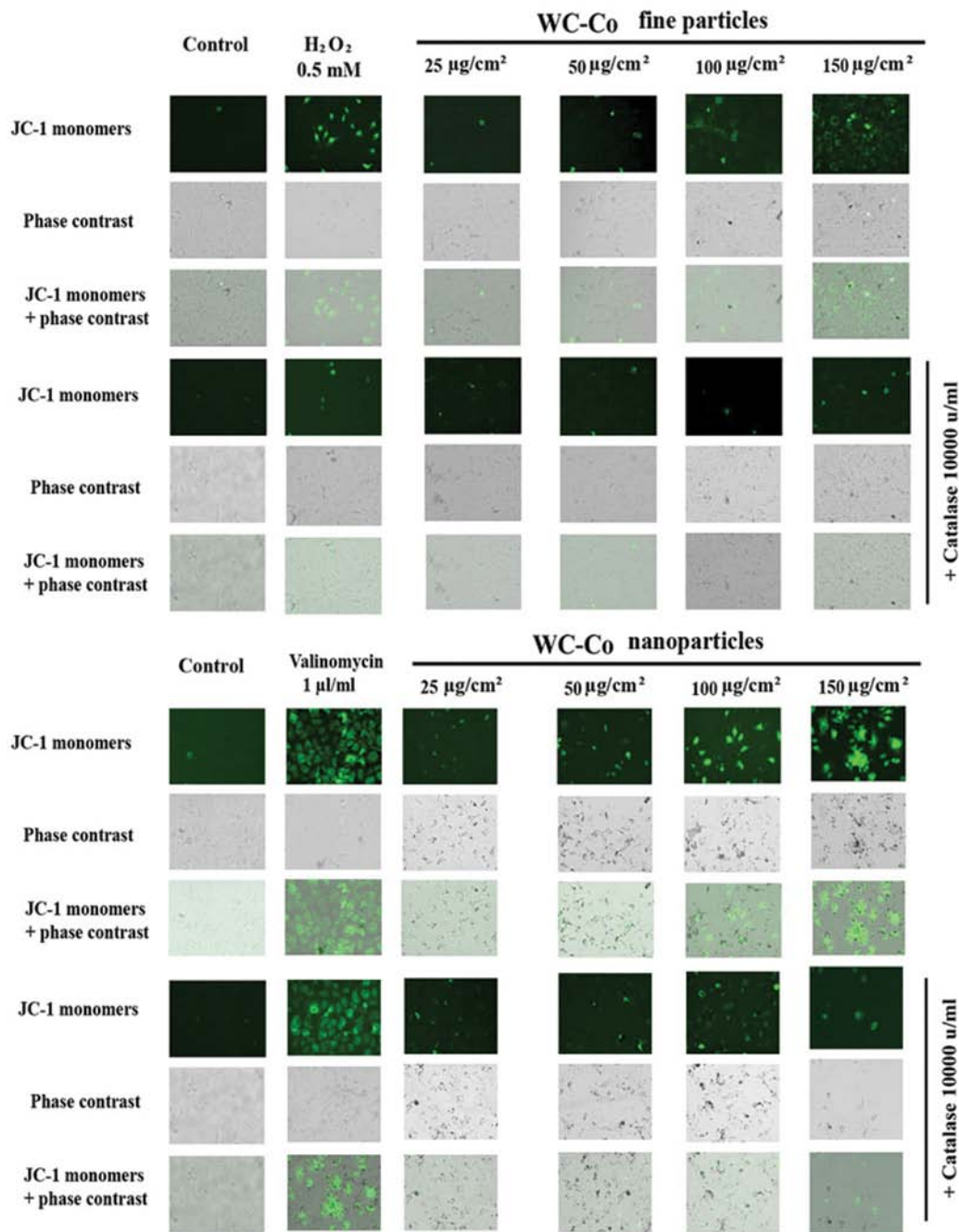
Figure 5. Effect of catalase on WC-Co particle-induced mitochondrial membrane permeability alteration. JB6 cells were seeded onto a 24-well plate and incubated overnight. Cells were treated with or without WC-Co particles in presence or absence of catalase for 24 h. A mitochondrial staining kit was used to detect the mitochondrial membrane permeability. Hydrogen peroxide and valinomycin were used as positive controls. Catalase exhibited partial inhibition of mitochondrial membrane permeability damage induced by WC-Co particles and hydrogen peroxide, but not by valinomycin.

suggesting that the pulmonary toxicity might be mediated by surface effects. In the present study, surface area of WC-Co nanoparticles was 17-fold greater than fine particles. However, WC-Co nanoparticles exhibited potency for cytotoxicity and apoptosis induction which was somewhat less than 17-fold greater than fine particles. Therefore, in agreement with our previous study with $TiO_2$ particles (7), specific surface area measured by gas absorption, tends to over correct for the greater cytotoxicity probably because it over estimates the surface area of agglomerates.

Apoptosis and necrosis are two forms of cell death that have been defined on the basis of distinguishable, morphological criteria (36). Apoptosis is a programmed cell death which is now widely recognized as being of critical importance in health and disease. Although studies have demonstrated that WC-Co fine particles induce cell apoptosis (2,9), the molecular pathways have not been well investigated. Our results suggest that, after 24-h treatment, both WC-Co nano- and fine particles induce JB6 apoptosis in a dose response manner within a certain dose range. Further studies revealed that treatment with
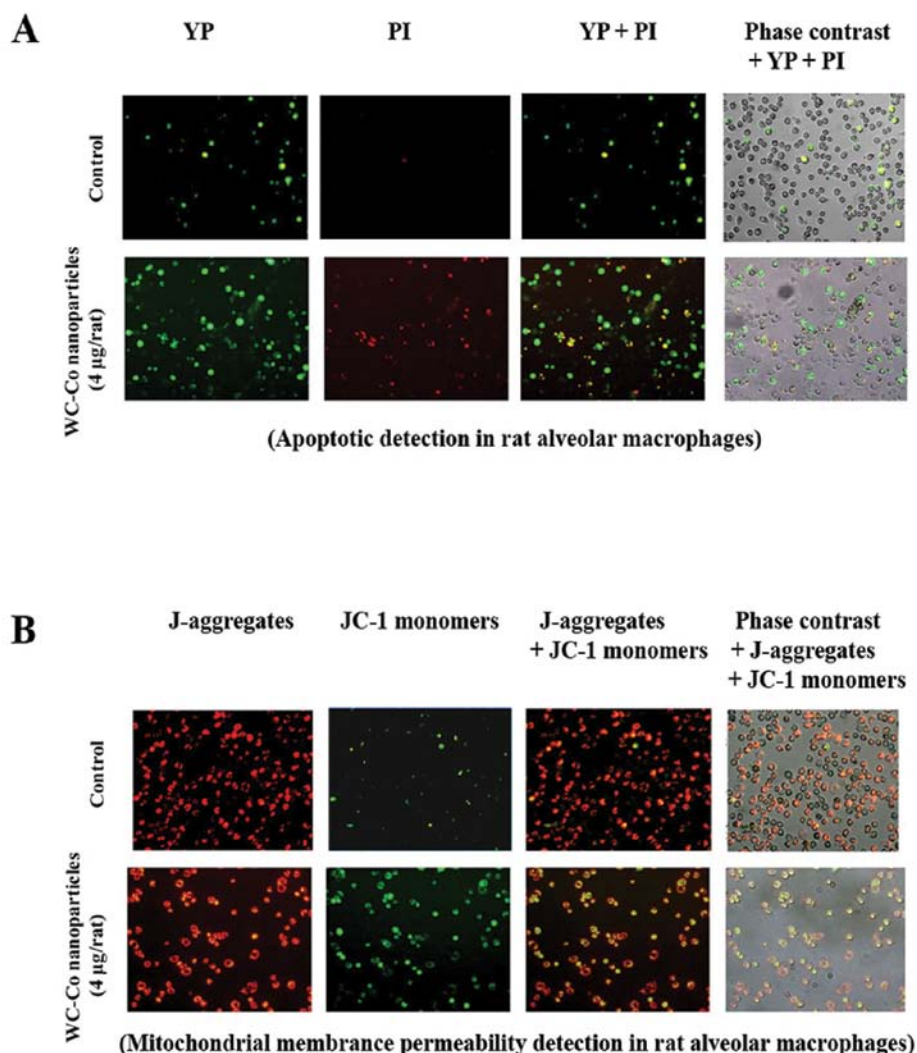
Figure 6. Apoptosis and mitochondrial membrane permeability alteration induced by WC-Co nanoparticles in rat lung macrophages. (A) Apoptosis induced by WC-Co nanoparticles in rat lung macrophages. Apoptotic cells were positively stained by YP (green) alone. Late apoptotic or necrotic cells were positively stained by both YP (green) and PI (red). WC-Co nanoparticles induced more apoptotic cells than control. (B) WC-Co nanoparticles significantly induced mitochondrial membrane permeability damage in rat lung macrophages compared to control.

WC-Co nanoparticles by intranasal droplet application induced both apoptosis and necrosis (or late apoptosis) in rat lung macrophages. Tozawa *et al* reported with a single intratracheal administration, WC-Co dusts induced marked fibrotic changes in rat pulmonary tissues after 6 months (37). Combined with our results, apoptosis or necrosis in rat lung macrophages induced by WC-Co nanoparticles may play an important role in the formation of the experimental pneumoconiosis (37).

In mammals, signaling cascades culminating in apoptotic cell death can be divided into intrinsic or extrinsic pathways. The extrinsic pathway is initiated upon activation of death receptors. The intrinsic pathway can be initiated by cellular stresses, such as cytochrome *c* release from mitochondria into the cytoplasm. In this study, WC-Co particles induced Fas, FADD upregulation and caspase 8 activation. These results imply that in the apoptotic process induced by WC-Co particles, the extrinsic signal pathway is initiated. To investigate the involvement of intrinsic pathways in the apoptotic process induced by WC-Co particles, AIF and cytochrome *c* release from mitochondria to the cyto-

plasm were examined. Our results show that WC-Co particles induced upregulation and release of AIF and cytochrome *c* from mitochondria to the cytoplasm. In addition, the mitochondrial permeability assay showed that WC-Co particles induced significant changes in the mitochondrial membrane permeability, which was in parallel with western blot results. These results indicate that the apoptotic process induced by WC-Co particles involves both intrinsic and extrinsic pathways.

Lamins are nuclear membrane structural components, which are important for maintaining normal cell functions. Proteolysis of lamins has been observed in different cells undergoing apoptosis (38). Degradation of lamina proteins can be triggered by both the extrinsic and the intrinsic pathways (39). Our results show that lamin A, but not C, was cleaved in cells treated with WC-Co nanoparticles, suggesting involvement of lamin A in the apoptotic process induced by WC-Co nanoparticles. The actin cytoskeleton is capable of responding to complex signaling cascades. The major cytoskeletal filament, actin, can be degraded during the execution phase of apoptosis (40). Reports indicate

that disruption of actin filament integrity promptly induces apoptosis in adherent epithelial cells (41). In addition, the dynamic state of actin is important in the regulation of ion channels (42). In the present study, WC-Co particles induced β-actin cleavage after 1-h treatment in JB6 cells. These results, combined with our previous study with metallic nickel particles (7) and a report by White *et al* (41), suggest that the actin cytoskeletal network may act as a target for apoptosis and an early signaling component toward apoptotic commitment in the apoptotic process induced by metallic particles.

The Bcl-2 proteins are a family of proteins involved in the response to apoptosis. Some of these proteins, such as BAX and BID, are proapoptotic, while others, such as Bcl-2, are anti-apoptotic. In the present study, WC-Co particles induced both proapoptotic factors of BAX and BID and anti-apoptotic factor of Bcl-2, especially in nanoparticle-treated cells. Increased Bcl-2 may antagonize the effects of activated BID on the translocation of cytochrome *c* (7). In addition, Bcl-2 activation may provide the necessary conditions for the selection of cells that have become resistant to apoptosis, which may also be important in the WC-Co-induced carcinogenic process. Therefore, further research is needed to elucidate the role of activation of Bcl-2 in the carcinogenicity of WC-Co particles.

Mitochondrial dysfunction has been shown to participate in the induction of apoptosis. Changes in the mitochondrial membrane permeability are considered early events in apoptosis (43). Many proapoptotic proteins, including cytochrome *c*, AIF, heat shock proteins, Smac/Diablo, and endonuclease G, can be released from the mitochondria into the cytoplasm following the formation of a pore in the mitochondrial membrane (44). AIF is involved in initiating a caspase-independent pathway of apoptosis by causing DNA fragmentation and chromatin condensation (45). However, cytochrome *c* induces apoptosis in a caspase-dependent pathway (46). In this study, WC-Co particles, especially nanoparticles, induced a significant increase in the mitochondrial membrane permeability in JB6 cells after 24-h treatment and release of cytochrome *c* and AIF from mitochondria into cytoplasm. In addition, lung macrophages from rats exposed to WC-Co nanoparticles by intranasal droplet application (4 g/rat) for 21 days exibited significant mitochondrial membrane permeability alteration in rat lung macrophages. These results indicate that the intrinsic mitochondrial pathway is involved in WC-Co particle-induced apoptosis.

Caspases, a family of aspartic acid-specific proteases, are the major effectors of apoptosis. The execution of apoptosis comprises both caspase-dependent and caspase-independent processes. In the present study, WC-Co particles significantly activated caspase 3 and 8. Caspase 9 was slightly activated. Taken together, our results suggest that apoptosis induced by WC-Co particles in JB6 cells involves both caspase-dependent and caspase-independent pathways.

In conclusion, the major findings of the present study show that both WC-Co nano- and fine particles induced JB6 cell and rat lung macrophage apoptosis. WC-Co nanoparticles elicited higher cytotoxicity and apoptotic induction than fine particles. WC-Co particles stimulated ROS generation in JB6 cells and rat lung macrophages. Catalase exhibited partly inhibitory effects on WC-Co particle-induced ROS generation and mitochondrial membrane permeability damage. To our knowledge, this is the first study showing that WC-Co particles activated both extrinsic and intrinsic apoptotic pathways in JB6 cells, which include upregulation of Fas, FADD, caspase 3, 8 and 9, BAX and BID, as well as release of AIF and cytochrome *c* from mitochondria into the cytoplasm. Lamin A and β-actin were cleaved. Furthermore, an increase of mitochondrial membrane permeability was observed in both WC-Co particle-treated JB6 cells and rat lung macrophages. On a mass basis, WC-Co nanoparticles exhibited higher cytotoxicity and apoptotic induction than fine particles. Particle size may play a critical role in the toxicity of this hard metal. Specific surface area tends to overcorrect for the greater toxicity when comparing the cytotoxicity of WC-Co nano- with fine particles. Apoptosis induced by WC-Co nano- and fine particles in JB6 cells may be mediated through ROS generation.

## Acknowledgements

## References

1. Dagani R: Nanostructured materials promise to advance range of technologies. Chem Engineer News 23: 18-24, 1992.
2. Lombaert N, Lison D, Van Hummelen P and Kirsch-Volders M: In vitro expression of hard metal dust (WC-Co) - responsive genes in human peripheral blood mononucleated cells. Toxicol Appl Pharmacol 227: 299-312, 2008.
3. Driscoll KE, Maurer JK, Lindenschmidt RC, Romberger D, Rennard SI and Crosby L: Respiratory tract responses to dust: relationships between dust burden, lung injury, alveolar macrophage fibronectin release, and the development of pulmonary fibrosis. Toxicol Appl Pharmacol 106: 88-101, 1990.
4. Oberdorster G, Ferin J and Lehnert BE: Correlation between particle size, in vivo particle persistence, and lung injury. Environ Health Perspect 102 (Suppl 5): 173-179, 1994.
5. Oberdorster G: Pulmonary effects of inhaled ultrafine particles. Int Arch Occup Environ Health 74: 1-8, 2001.
6. Zhao J, Bowman L, Zhang X, *et al*: Titanium dioxide (TiO2) nanoparticles induce JB6 cell apoptosis through activation of the caspase-8/Bid and mitochondrial pathways. J Toxicol Environ Health A 72: 1141-1149, 2009.
7. Zhao J, Bowman L, Zhang X, *et al*: Metallic nickel nano- and fine particles induce JB6 cell apoptosis through a caspase-8/AIF mediated cytochrome c-independent pathway. J Nanobiotechnol 7: 2, 2009.
8. Pulido MD and Parrish AR: Metal-induced apoptosis: mechanisms. Mutat Res 533: 227-241, 2003.
9. Lombaert N, De Boeck M, Decordier I, Cundari E, Lison D and Kirsch-Volders M: Evaluation of the apoptogenic potential of hard metal dust (WC-Co), tungsten carbide and metallic cobalt. Toxicol Lett 154: 23-34, 2004.
10. Raff MC: Social controls on cell survival and cell death. Nature 356: 397-400, 1992.
11. Steller H: Mechanisms and genes of cellular suicide. Science 267: 1445-1449, 1995.
12. White E: Life, death, and the pursuit of apoptosis. Genes Dev 10: 1-15, 1996.
13. Wyllie AH, Kerr JF and Currie AR: Cell death: the significance of apoptosis. Int Rev Cytol 68: 251-306, 1980.

14. Lu X, Lee M, Tran T and Block T: High level expression of apoptosis inhibitor in hepatoma cell line expressing Hepatitis B virus. Int J Med Sci 2: 30-35, 2005.
15. Ramp U, Krieg T, Caliskan E, et al: XIAP expression is an independent prognostic marker in clear-cell renal carcinomas. Hum Pathol 35: 1022-1028, 2004.
16. Kuwano K, Miyazaki H, Hagimoto N, et al: The involvement of Fas-Fas ligand pathway in fibrosing lung diseases. Am J Respir Cell Mol Biol 20: 53-60, 1999.
17. Bardales RH, Xie SS, Schaefer RF and Hsu SM: Apoptosis is a major pathway responsible for the resolution of type II pneumocytes in acute lung injury. Am J Pathol 149: 845-852, 1996.
18. Levine AJ: p53, the cellular gatekeeper for growth and division. Cell 88: 323-331, 1997.
19. Matute-Bello G, Winn RK, Jonas M, Chi EY, Martin TR and Liles WC: Fas (CD95) induces alveolar epithelial cell apoptosis in vivo: implications for acute pulmonary inflammation. Am J Pathol 158: 153-161, 2001.
20. McCabe MJ Jr: Mechanisms and consequences of silica-induced apoptosis. Toxicol Sci 76: 1-2, 2003.
21. Gawlitta D, Oomens CW, Baaijens FP and Bouten CV: Evaluation of a continuous quantification method of apoptosis and necrosis in tissue cultures. Cytotechnology 46: 139-150, 2004.
22. Boffa DJ, Waka J, Thomas D, et al: Measurement of apoptosis of intact human islets by confocal optical sectioning and stereologic analysis of YO-PRO-1-stained islets. Transplantation 79: 842-845, 2005.
23. Ding M, Kisin ER, Zhao J, et al: Size-dependent effects of tungsten carbide-cobalt particles on oxygen radical production and activation of cell signaling pathways in murine epidermal cells. Toxicol Appl Pharmacol 241: 260-268, 2009.
24. Grossmann J, Mohr S, Lapentina EG, Fiocchi C and Levine AD: Sequential and rapid activation of select caspases during apoptosis of normal intestinal epithelial cells. Am J Physiol 274: G1117-G1124, 1998.
25. Okinaga T, Kasai H, Tsujisawa T and Nishihara T: Role of caspases in cleavage of lamin A/C and PARP during apoptosis in macrophages infected with a periodontopathic bacterium. J Med Microbiol 56: 1399-1404, 2007.
26. Mashima T, Naito M and Tsuruo T: Caspase-mediated cleavage of cytoskeletal actin plays a positive role in the process of morphological apoptosis. Oncogene 18: 2423-2430, 1999.
27. Caroppi P, Sinibaldi F, Fiorucci L and Santucci R: Apoptosis and human diseases: mitochondrion damage and lethal role of released cytochrome C as proapoptotic protein. Curr Med Chem 16: 4058-4065, 2009.
28. Susin SA, Lorenzo HK, Zamzami N, et al: Molecular characterization of mitochondrial apoptosis-inducing factor. Nature 397: 441-446, 1999.
29. Susin SA, Daugas E, Ravagnan L, et al: Two distinct pathways leading to nuclear apoptosis. J Exp Med 192: 571-580, 2000.
30. Piacenza L, Irigoin F, Alvarez MN, et al: Mitochondrial superoxide radicals mediate programmed cell death in Trypanosoma cruzi: cytoprotective action of mitochondrial iron superoxide dismutase overexpression. Biochem J 403: 323-334, 2007.
31. Long TC, Tajuba J, Sama P, et al: Nanosize titanium dioxide stimulates reactive oxygen species in brain microglia and damages neurons in vitro. Environ Health Perspect 115: 1631-1637, 2007.
32. Lison D: Human toxicity of cobalt-containing dust and experimental studies on the mechanism of interstitial lung disease (hard metal disease). Crit Rev Toxicol 26: 585-616, 1996.
33. Kear BH, Skandan G and Sadangi RK: Factors controlling decarburization in HVOF sprayed nano-WC/Co hardcoatings. Scripta Materialia 44: 1703-1707, 2001.
34. Busch W, Kuhnel D, Schirmer K and Scholz S: Tungsten carbide cobalt nanoparticles exert hypoxia-like effects on the gene expression level in human keratinocytes. BMC Genomics 11: 65, 2010.
35. IARC Working Group on the Evaluation of Carcinogenic Risks to Humans: Cobalt in hard metals and cobalt sulfate, gallium arsenide, indium phosphide and vanadium pentoxide. IARC Monogr Eval Carcinog Risks Hum 86: 1-294, 2006.
36. Helewski KJ, Kowalczyk-Ziomek GI and Konecki J: Apoptosis and necrosis - two different ways leading to the same target. Wiad Lek 59: 679-684, 2006 (In Polish).
37. Tozawa T, Kitamura H, Koshi K, Ikemi Y and Ambe K: Experimental pneumoconiosis induced by cemented tungsten and sequential concentrations of cobalt and tungsten in the lungs of the rat. Sangyo Igaku 23: 216-226, 1981 (In Japanese).
38. Goldberg M, Harel A and Gruenbaum Y: The nuclear lamina: molecular organization and interaction with chromatin. Crit Rev Eukaryot Gene Expr 9: 285-293, 1999.
39. Broers JL, Bronnenberg NM, Kuijpers HJ, Schutte B, Hutchison CJ and Ramaekers FC: Partial cleavage of A-type lamins concurs with their total disintegration from the nuclear lamina during apoptosis. Eur J Cell Biol 81: 677-691, 2002.
40. Janmey PA: The cytoskeleton and cell signaling: component localization and mechanical coupling. Physiol Rev 78: 763-781, 1998.
41. White SR, Williams P, Wojcik KR, et al: Initiation of apoptosis by actin cytoskeletal derangement in human airway epithelial cells. Am J Respir Cell Mol Biol 24: 282-294, 2001.
42. Gourlay CW and Ayscough KR: The actin cytoskeleton: a key regulator of apoptosis and ageing? Nat Rev Mol Cell Biol 6: 583-589, 2005.
43. Ly JD, Grubb DR and Lawen A: The mitochondrial membrane potential (deltapsi(m)) in apoptosis; an update. Apoptosis 8: 115-128, 2003.
44. Siskind LJ, Kolesnick RN and Colombini M: Ceramide forms channels in mitochondrial outer membranes at physiologically relevant concentrations. Mitochondrion 6: 118-125, 2006.
45. Landshamer S, Hoehn M, Barth N, et al: Bid-induced release of AIF from mitochondria causes immediate neuronal cell death. Cell Death Differ 15: 1553-1563, 2008.
46. Garland JM and Rudin C: Cytochrome c induces caspase-dependent apoptosis in intact hematopoietic cells and overrides apoptosis suppression mediated by bcl-2, growth factor signaling, MAP-kinase-kinase, and malignant change. Blood 92: 1235-1246, 1998.